Core-substituted naphthalenediimides

Naomi Sakai,*[a] Jiri Mareda,[a] Eric Vauthey[b] and Stefan Matile*[a]

Received 23rd February 2010, Accepted 7th April 2010
First published as an Advance Article on the web 14th May 2010
DOI: 10.1039/c0cc00078g

This *feature article* reviews research of core-substituted naphthalenediimides (cNDIs) in a comprehensive yet easily readable manner. Their synthesis, electrochemistry and spectroscopy are covered first with emphasis on the ability of cNDIs with electron donating substituents to absorb and fluoresce in all colors without global structural changes and cNDIs with electron withdrawing substituents to reach unprecedented extents of π-acidity. The section on supramolecular chemistry covers face-to-face π-stacks and peripheral hydrogen bonds, that on molecular recognition moves from pH and fluoride sensors to the binding to telomeric DNA *in vivo* and intercalation into π-stacks and sticky tweezers. cNDIs can recognize and transport anions by functional anion–π interactions. The section on electron transport describes cNDIs as air-stable n-semiconductors with high charge mobility and use as OFETs. Photoinduced electron transport by rainbow cNDIs has been used for the creation of artificial photosystems in solution, in bilayer membranes and on solid substrates. Examples include multicolor light harvesting architectures, organic solar cells, photosystems that can open up into ion channels, and supramolecular n/p-heterojunctions with antiparallel redox gradients. The review is highly interdisciplinary but should appeal most to organic, biosupramolecular and physical chemists.

Introduction

In this review, recent progress with core-substituted naphthalenediimides (cNDIs, **1**) is summarized in a quite comprehensive manner. cNDIs are 1,4,5,8-naphththalenediimides (NDIs, **2**) with one or more substituents in position 2, 3, 6 and 7 (Fig. 1). With electron donors in the core, cNDIs become colorful push–pull systems, whereas electron acceptors produce exceptionally π-acidic aromatic systems.

Although known since a very long time,[1] research on cNDIs has really taken off only with recent improvements on synthetic access[2–7] and the discovery of rainbow fluorescence,[2] electron transport[6] and anion binding.[7] The closest relatives of cNDIs are much better explored (Fig. 1). The parent NDI **2**, for example, has been used extensively as an electron acceptor, n-semiconductor and intercalator in aromatic donor–acceptor complexes, molecular tweezers, catenanes, foldamers, gels, nanotubes, ion channels, pores, and optoelectronic devices. This research has been reviewed recently.[8]

Also cPDIs **3**, the big brother of cNDIs, are much better explored, presumably because their synthesis is better established.[9] Compared to the twisted cPDIs, cNDIs are planar. This planarity is important for ordered π-stack architectures with high conductivity. Moreover, cNDIs are more compact and colorizable over the whole visible range, whereas unsubstituted PDIs **4** already absorb around 530 nm.[9] Fragments of NDIs can be seen in naphthalene monoimides **5** and phthaldiimide **6**.[10] High π-acidity makes cNDIs with

[a] *Department of Organic Chemistry, University of Geneva, Geneva, Switzerland. E-mail: stefan.matile@unige.ch, naomi.sakai@unige.ch; Fax: +41 22 379 5123; Tel: +41 22 379 6523; Web: www.unige.ch/sciences/chiorg/matile/*
[b] *Department of Physical Chemistry, University of Geneva, Geneva, Switzerland*

Naomi Sakai

Naomi Sakai obtained her BS from Keio University (1987) and her PhD from Tokushima Bunri University (1994). Since a postdoc at Columbia University with Professor Koji Nakanishi (1994–1996), she has focused on supramolecular functional architectures for applications such as solar cells and biosensors, first in Washington DC (Georgetown University, 1996–1999), then in Geneva (1999–present).

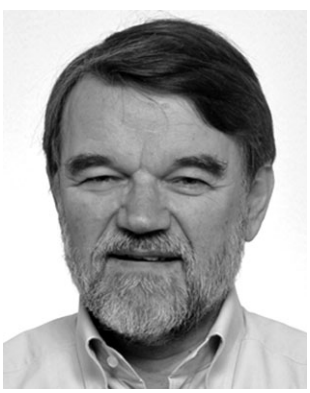

Jiri Mareda

Jiri Mareda obtained both his Diploma (1975) and PhD (1980) from the University of Geneva, where he worked under the supervision of Professors C. W. Jefford and U. Burger. During a post-doctoral stay with Professor Ken Houk (1980–1983) he specialized in computational chemistry, which he applied in organic, bioorganic and supramolecular chemistry after returning to Geneva University.

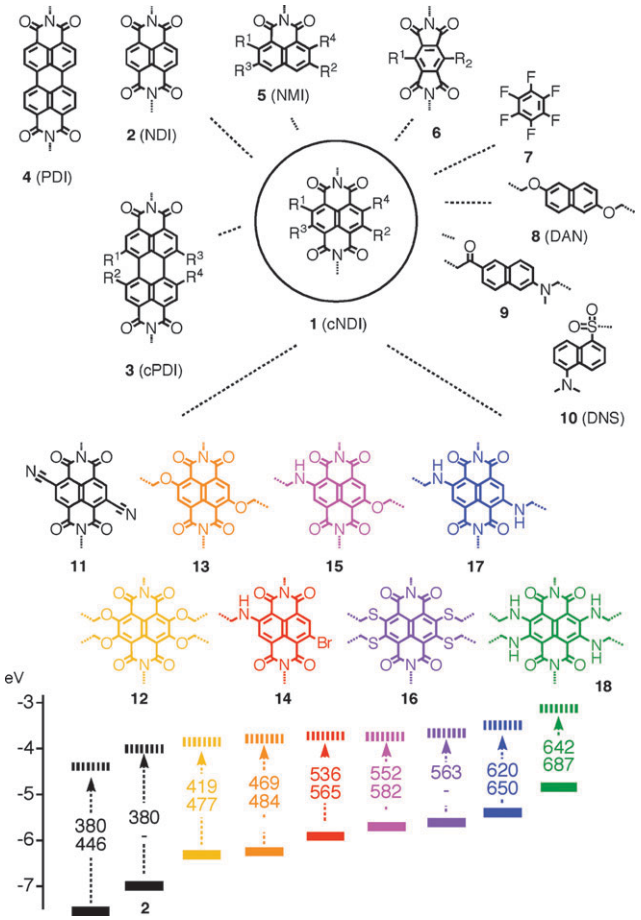

Fig. 1 Core-substituted naphthalenediimides **1**, related structures **2–10** and a rainbow collection **11–18** with indication of HOMO (bold) and LUMO (dashed) energies in eV against vacuum and maximal absorption (top) and emission wavelength (bottom) in nm.

withdrawing substituents similar to the archetypal hexafluorobenzene **7**.[11] The complementary donating substituents relate cNDIs to π-basic classics such as the dialkoxynaphthyls **8** (DANs) that are often used as NDI partners in charge-transfer stacks.[8,12] The combination of donating substituents in the core with withdrawing imides gives versatile push–pull chromophores with similarities to laurdan **9**, a famous two-photon probe for membrane microdomains,[13] or the classical dansyl **10** (DNS) known *inter alia* from peptide sequencing.[14] The ability of cNDIs to change color and redox properties is arguably their most attractive characteristic.[2,15] The rainbow collection **11–18** perfectly illustrates how the HOMO–LUMO-gaps decrease while HOMO and LUMO energies increase with increasingly donating substituents in the core.[15] The replacement of single atoms is sufficient to cover the primary colors, moving from yellow, green-fluorescent cNDI **13** with two oxygens over the red, orange-fluorescent cNDI **15** with one oxygen and one nitrogen to the blue, red-fluorescent cNDI **17** with two nitrogens in the core. The compact cNDI **17** is probably the smallest, most ''atom-efficient'' chlorophyll mimic known today.[16]

In the following, we first summarize synthesis, electrochemistry, spectroscopy and supramolecular chemistry of cNDIs. This part is followed by a summary of applications of cNDIs to molecular recognition, anion transport and electron transport to close with photoinduced electron transport in artificial photosystems. Before moving on, we point out that according to IUPAC, cNDIs are 1,2,3,6,7,8-hexahydrobenzo-[*lmn*][3,8]phenanthroline-1,3,6,8-tetraones with substituents in position 4, 5, 9 and/or 10; naphthalene bisimide, naphthalene diimide and naphthalenediimide are the most frequently used trivial names.

Synthesis

The traditional approach to cNDIs starts with the oxidation of pyrene **19** (Scheme 1).[1,2] The four-step protocol includes strong acids such as fuming HNO_3, strong bases and chlorine gas. The resulting dianhydride **20** with two chlorides in the core is then converted to diimide **21** by reacting with amines in AcOH to prevent core substitution. From diimide **21**, cNDIs are accessible by nucleophilic aromatic substitution.

Eric Vauthey

Eric Vauthey graduated in chemistry and obtained his PhD in physical chemistry at the University of Fribourg in Switzerland. After two post-doctoral stays, one at the Royal Institution and the Imperial College in London, and the other at the ETH in Zurich, he returned to Fribourg in 1992 and started an independent research on the development and the applications of optical spectroscopy for investigating of ultrafast photoinduced processes in liquids and at interfaces. He is presently pursuing this research at the University of Geneva since his appointment as professor of physical chemistry in 2001.

Stefan Matile

Stefan Matile obtained his MS (1989) and PhD (1994) from the University of Zurich under the supervision of Wolf Woggon. He was a postdoc with Koji Nakanishi at Columbia University in New York (1994–1996) and Assistant Professor at Georgetown University, Washington DC before moving to Geneva (1999). His research interests are at the interface of synthetic organic, biological and supramolecular materials chemistry (photosystems, biosensors, ion channels).

This journal is © The Royal Society of Chemistry 2010

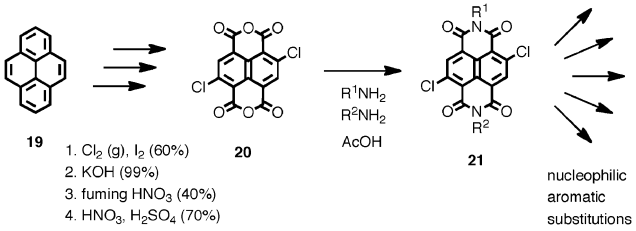

Scheme 1 A traditional approach to cNDIs.

The classical entry to cNDIs has been discouraging because of the harsh conditions of the initial pyrene oxidation, particularly for academic labs. To avoid reagents such as chlorine gas in large amounts, alternative routes to cNDIs have been developed recently (Scheme 2).[3–7] In this attractive approach, the commercially available dianhydride **22** is brominated with dibromocyanuric acid **23**. The resulting product mixture containing **24** is directly carried on to the diimide formation with amines under acidic conditions. Isolation and purification of the resulting 2,6-dibromo cNDI **25** is unproblematic.

From this key intermediate, a broad variety of cNDIs is accessible by nucleophilic aromatic substitution. This includes dicyano cNDIs **11**[6,7] or red cNDIs **14** and blue cNDIs **17** with one or two alkylamines in the core, respectively.[2–5] The facile introduction of the first amine illustrates perfectly the electron deficiency of the naphthalene in cNDIs, while the more demanding introduction of the second amine reflects the reduction of this deficit by one amine donor in **14**.

Suzuki–Miyaura coupling with boronate esters **26** gives cNDIs **27** with phenyls in the core.[17] Steric hindrance prevents π-conjugation with the NDI core and twists the phenyls out of plane. This lack of conjugation can be overcome by inserting a triple bonds *via* Stille coupling with tin reagents such as **28** to

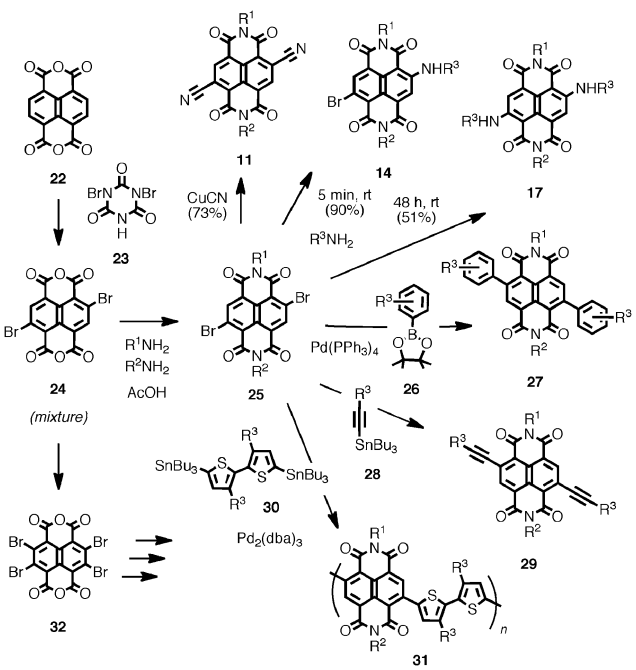

Scheme 2 An alternative approach to cNDIs.

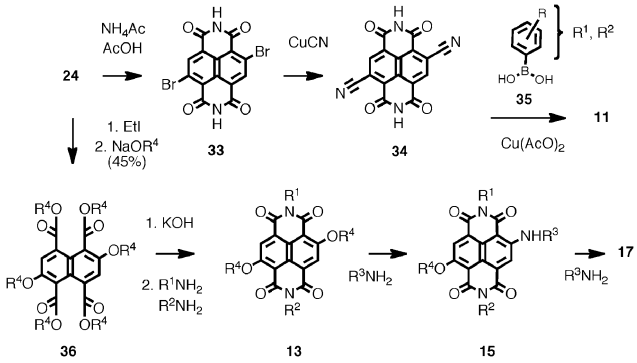

Scheme 3 Problem solving in cNDI synthesis.

give cNDIs **29**, which in turn can be activated for transition-metal catalyzed coupling with aromatics.[18] The same chemistry has been used to attach difunctionalized, electron-rich bithiophenes **30** for the preparation of polymers **31**.[19]

This facile approach to cNDIs *via* dibromo cNDI **25** is robust and general. It has led to an increasing number of publications on cNDIs from an increasing number of different groups over the past few years. Tetrasubstituted cNDIs are accessible *via* tetrabromo dianhydrides **32** prepared with an excess of brominating agent **23**, followed by diimide formation and nucleophilic aromatic substitution.[20–22]

The development of problem-solving strategies has proven possible in several cases (Scheme 3). For instance, the suppression of competing core substitution during the formation of diimide **25** has been problematic for a few aromatic amines with poor basicity. In this case, free diimides **33** were prepared first with ammonium acetate in refluxing acetic acid in good ~80% yield. After introduction of the desired core substituents, the peripheral substituents were then attached in the last step by copper-catalyzed coupling of the free diimides **34** with aryl boronic acids **35**.[7,23]

Another example concerns the yellow cNDIs **13**. This chromophore can be prepared by treating cNDI **25** with alcoholate, which however is often incompatible with interesting functional groups in the peripheral sidechains R^1 and R^2. This problem was solved by opening dianhydride **24** into the tetraethylester before exposure to the alcoholate for core substitution.[5] The transesterification that naturally occurs under these conditions is irrelevant because the obtained tetraester **36** is hydrolyzed anyway before the formation of yellow cNDIs **13** with the amines of choice. In an exceptionally colorful reaction, one alkoxy substituent in the yellow cNDIs **13** can be replaced by an alkylamino substituent to give the pink cNDIs **15** which, if desired, can react under slightly harsher conditions with another amine to give the blue cNDIs **17**.[24]

Electrochemistry

The energy levels of the frontier molecular orbitals of cNDIs can be estimated by cyclic voltammetry (CV), complemented, if necessary, by differential pulse voltammetry, absorption and fluorescence spectroscopy.[15] The onset of the first reduction of NDIs **2** occurs at −0.81 V against the ferrocene/ferrocenium

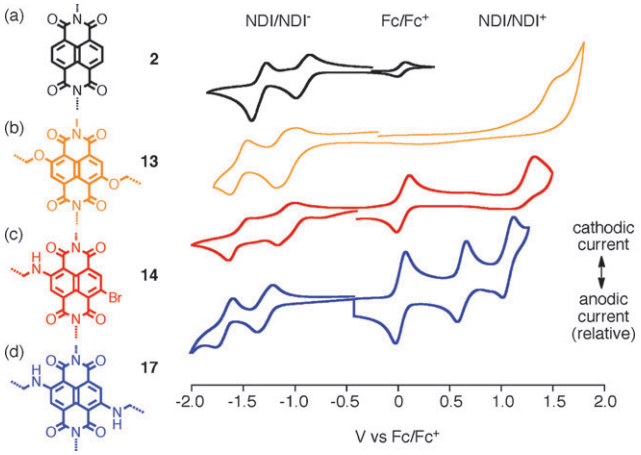

Fig. 2 Cyclic voltammograms of cNDIs **13** (b), **14** (c), **17** (d) compared to unsubstituted NDIs **2** (a) with Fc/Fc^+ as internal standard. Adapted with permission from ref. 15. Copyright 2009, American Chemical Society.

couple (Fig. 2a). As the second reduction at −1.1 V and most redox processes of cNDIs, this reduction is reversible. Subtraction of the −4.8 eV for Fc/Fc^+ against vacuum places the LUMO of unsubstituted NDIs **2** at −4.01 eV against vacuum (Fig. 1). The oxidation of NDIs **2** was not detectable (Fig. 2a). The HOMO energy (−7.07 eV, Fig. 1) has thus to be determined from the LUMO level minus the HOMO/LUMO gap available from absorption spectra (see below).

The introduction of the two alkoxy donors in the core of yellow cNDIs **13** raises the LUMO to −3.82 eV, and the first oxidation accounting for the HOMO level of −6.16 eV can be determined directly by CV (Fig. 2b and 1). Replacement of one alkoxy donor with a stronger alkylamine in the cNDIs **15**[24] further raises both HOMO and LUMO to levels that are close to that of the halogenated cNDIs **14**, (Fig. 2c). Replacement of both alkoxy donors with alkylamines in cNDIs **17** raises the HOMO energies to −5.35 eV and LUMO levels to −3.56 eV (Fig. 1). The CV confirms that the blue cNDIs **17** can be easily and reversibly oxidized up to the dication, whereas similarly facile and reversible reduction to the dianion remains possible as well (Fig. 2d). These unique redox properties make cNDIs **17** similar to chlorophyll and very attractive for optoelectronic applications (see below). A comprehensive list of HOMO and LUMO energies of the cNDIs available today, *i.e.*, **11–18** and **25–82**, can be found in Table 1. Important examples will be discussed together with spectroscopic properties.

Spectroscopy

The ability to change both color and redox properties without global structural changes is the most attractive characteristics of cNDIs.[2,15] The representative absorption and fluorescence spectra in Fig. 3 show that the π–π*-transition with its characteristic vibrational fine structure around 380 nm is not sensitive to core-substitution.[15] The color of cNDIs originates from a new charge-transfer band that moves to the red over the full rainbow with increasing push–pull character of the cNDI. This decreasing "bandgap" with increasing HOMO and LUMO energies is rare and very attractive for applications (Fig. 1).[15,25]

With electron donating core substituents, bandgaps decrease from ethers over sulfides[20,26] and selenides[26] toward amines.[2,15,26–30] Tertiary amines without hydrogen-bond donor to the imide carbonyls do not fluoresce (**47**, Table 1, entry 20).[18] 2,3-Diamines do not cause the same red-shift as 2,6-amines (**48**, Table 1, entry 21).[28,29] However, extended conjugation in 2,3-diamine **50** pushes the absorption maximum to 615 nm.[30] 2,3,5-Triamine **51** absorbs at 579 nm with very strong red-emission at 605 nm, and cyclic and acyclic tetra-amines **54** and **18** reach 629 and 642 nm with preserved yet weakened fluorescence, respectively (Table 1, entries 23–27).[20] The bandgap of **18** is slightly smaller and the HOMO/LUMO levels are slightly higher than in chlorophyll.[20]

Core-substitution with C–C bonds in **55–74** gives generally weaker spectroscopic shifts.[17,18,31,32] Spectacular exceptions include conjugated systems such as the extended diamine **55**, absorbing at 692 nm with HOMO/LUMO levels remaining to the range of normal diamines **17** (Table 1, entry 28).[18] Moreover, mono-, di- and terthiophene donors in the cNDI core of **72–74** push the absorption to 664 nm (Table 1, entries 45–47, cNDI-oligothiophene and related polymers **75–82** will be covered in a separate chapter).[32]

The discovery of fluorescent cNDIs has, together with progress in organic synthesis, triggered the recent renaissance of cNDI research (Fig. 3a, dotted lines, Table 1, entries 8–27).[2] Unlike earlier reported non-fluorescent aryl-heteroatom-substituted cNDIs (Table 1, entries 5–7),[1,26] alkyl-heteroatom-substituted cNDIs could be highly fluorescent with their quantum yields reaching 76% for red cNDI **15** (Table 1, entry 13). Usefulness for single-molecule fluorescence has been confirmed for blue cNDIs **17** with "on" periods being detectable beyond 100 s.[27] Contrary to the heteroatom-bridged aryl substituents, many of the directly C–C coupled aryl substituents cause strong fluorescence.[17]

The circular dichroism (CD) spectra of monomeric cNDIs are naturally rather weak. In chiral dimers and stacks, stronger, bisignate exciton-coupled CD (ECCD) can be observed.[37] For example, the ECCD spectra of a helical stack of blue cNDIs **17** show negative doublets which disappear upon denaturation or untwisting of the helix into barrel-stave architectures with parallel NDI transition moments. Poorly understood and worth investigating on a fundamental level, these ECCD signals can be used to study self-assembly and self-organization, and to determine the absolute sense of twist in helical architectures (*M*-helicity in the case of Fig. 3b).[37]

The transient absorption (TA) spectra of monomeric cNDIs such as **17** observed a few picoseconds after a short femto-second laser pulse show usual effects such as ground-state bleaching, stimulated emission and excited state absorption (Fig. 3c, dotted).[16] The TA spectra of dimers and π-stacks of blue cNDIs **17** can look very different, with new absorptions appearing around 500 and 700 nm. These bands can be attributed to absorptions of the cNDI radical anion (Fig. 3c, solid). This means that after excitation, the electron in the LUMO can hop to a neighboring cNDI, producing a reduced NDI and leaving an oxidized cNDI behind. As with chlorophyll, the symmetry-breaking photoinduced charge separation with blue cNDIs **17** is attractive for optoelectronics applications because it occurs with minimal losses in photonic energy. The absorptions

This journal is © The Royal Society of Chemistry 2010

Table 1 Structure and optoelectronic properties of cNDIs

entry	compound		abs (ext)[a] em (QY)[b]	E_{red}[c] E_{ox}	LUMO[d] HOMO	ref
1	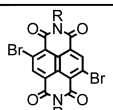	**25**	408 (16.5) -	-0.42[e] >1.6	-4.00 <-6.0	18
2	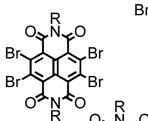	**32**	427(10.9) -	-0.75 +1.52	-4.05 -6.32	20, 22
3	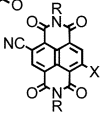 X = H	**37**	386 392	-0.22[e]	-4.20 -7.20	6
4	X = CN	**11**	380 446	+0.08[e]	-4.50 -7.50	6, 18
5	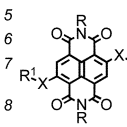 R[1] = aryl; X = O	**38**	462 (17.3)			26
6	X = S	**39**	519 (23.8)			26
7	X = NH	**40**	612 (22.8)	-1.38 +0.64	-3.42 -5.44	20, 26
8	R[1] = X = S	**41**	528 (21.7) 558			18
9	X = Se	**42**	553 (23.4) 594			18
10	X = S / NH	**43**	567 (24.3) 596			18
11	X = NH	**44**	610 (22.0) 642			18
12	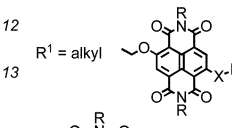 X = O	**13**	469 (18.2) 484 (22)	-0.98 +1.36	-3.82 -6.16	2, 15
13	R[1] = alkyl; X = NH	**15**	552 (17.7) 582 (76)	-1.25 +0.95	-3.75 -5.75	2, 24
14	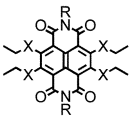 X = O	**12**	419 (12.2) 477 (2)	-1.27	-3.53	20
15	X = S	**16**	563 (15.4)	-1.10 +0.97	-3.70 +5.80	20
16	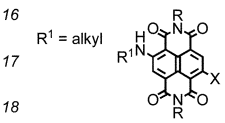 X = H	**45**	513 (11) 551 (51)			27
17	R[1] = alkyl; X = Cl	**46**	534 (15.6) 564 (64)	-1.02 +1.11	-3.78 -5.91	2, 3
18	X = Br	**14**	536 565 (32)	-0.95 +1.10	-3.85 -5.90	38
19	X = NHR[1]	**17**	620 (23.3) 650 (42)	-1.41 +0.65	-3.40 -5.45	3, 16
20	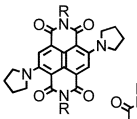	**47**	602 (22.0) 623 (0.2)	-1.03[e] +0.98	-3.37 -5.38	18
21	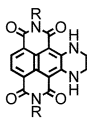	**48**	488 (32.6) 500 (42)			28, 29
22	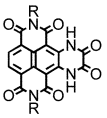	**49**	454 (base: 550) 465			29
23	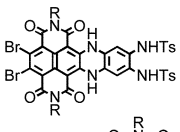	**50**	615 (F^-: 715) 635 (34)			30
24	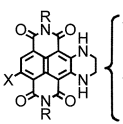 X = NHR[1]	**51**	579 (29.4) 605 (70)	-1.69 +0.41	-3.11 -5.21	21
25	R[1] = alkyl; X = OR[1]	**52**	511 (31.7) 521 (18)			21
26	X = Cl	**53**	497 (40) 500 (9)			21
26	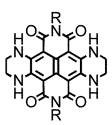	**54**	629 (36.0) 646 (19)	-1.85 -0.01	-2.95 -4.80	20
27	R[1] = alkyl 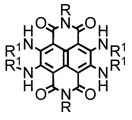	**18**	642 (26.5) 687 (13)	-1.69 +0.41	-3.11 -4.81	20

entry	compound		abs (ext)[a] em (QY)[b]	E_{red}[c] E_{ox}	LUMO[d] HOMO	ref
28	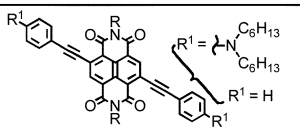 R[1] =	**55**	692 (49.4)	-0.57[e] +0.91	-3.83 -5.31	18
29	R[1] = H	**56**	494 (29.2) 528 (0.8)	-0.48[e] >1.6	-3.92 <6.0	18
30	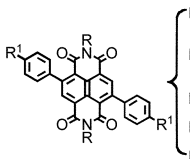 R[1] = CN	**57**	379 (17.7)	-0.43[e] >1.6	-3.97 <6.0	18
31	R[1] = Me	**58**	433 (9.3) 567 (41)	-1.05	-3.75	17
32	R[1] = F	**59**	418 (6.8)	-0.98	-3.82	17
33	R[1] = OMe	**60**	467 (8.4)	-1.02	-3.78	17
34	R[1] = CHO	**61**	514 (9.8)	-0.91	-3.89	17
35	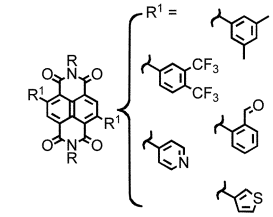 R[1] =	**62**	530 (7.8) 567 (47)	-1.15	-3.65	17
36		**63**	505 (5.4) 532 (51)	-0.92	-3.88	17
37		**64**	511 (7.4) 545 (58)	-0.68	-4.12	17
38		**65**	507 (2.3) 566 (62)	-0.93	-3.87	17
39		**66**	508 (1.1)	-1.07	-3.73	17
40	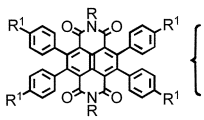 R[1] = H	**67**	377 (16.3)	-1.19	-3.61	31
41	R[1] = OMe	**68**	480 (6.2)	-1.26	-3.54	31
42	R[1] = CN	**69**	479 (19.4)	-0.92	-3.88	31
43	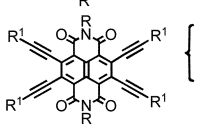 R[1] = Ph	**70**	535 (32.6) 560 (0.6)	-0.93	-3.87	31
44	R[1] = TMS	**71**	485 (44.0)	-0.97	-3.83	31
45	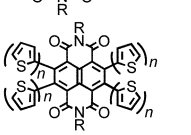 n = 1	**72**	514	-0.31[f] +1.80	-4.48 -6.60	32
46	n = 2	**73**	623	-0.30[f] +1.31	-4.50 -6.10	32
47	n = 3	**74**	664	-0.28[f] +1.29	-4.52 -6.09	32
48	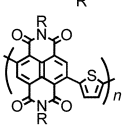	**75**	568	-0.97	-3.83 -5.49	33
49	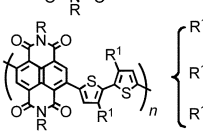 R[1] = H	**76**	693	-1.03	-3.77 -5.25	33, 34
50	R[1] = $C_{12}H_{25}$	**77**	539	-1.04	-3.76 -5.32	33
51	R[1] = $OC_{12}H_{25}$	**78**	985	-1.04	-3.76 -4.84	33
52	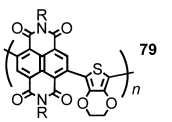	**79**	615	-0.55[e] +1.20	-3.85 -5.60	35
53	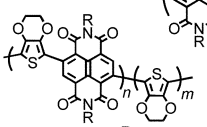	**80**	620/750	-0.61[e] +0.77	-3.79 -5.17	35
54	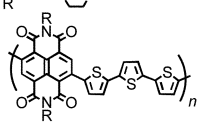	**81**	618	-0.44[f] +1.12	-3.94 -5.50	36
55	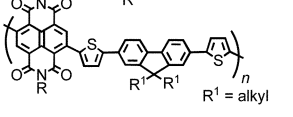 R[1] = alkyl	**82**	613 684 (1.1)	-0.52[f] +1.37	-3.86 -5.75	36

[a] Absorption maximum at low energy, with extinction coefficient in mM cm^{-1}. [b] Emission maximum, if applicable, with fluorescence quantum yield (QY) in %. [c] First oxidation and reduction potential in V against Fc/Fc^+. [d] LUMO and HOMO energies in eV against vacuum; from $E_{HOMO/LUMO} = -4.8$ eV (Fc) $- E_{red/ox}$ and $\Delta E_{HOMO/LUMO}{}^{opt} = 1240/\lambda_{max}{}^{onset}$ (nm). [e] In V against SCE; $E_{Fc} \approx E_{SCE} - 0.40$ V. [f] In V against Ag/AgCl; $E_{Fc} \approx E_{Ag} - 0.42$ V.

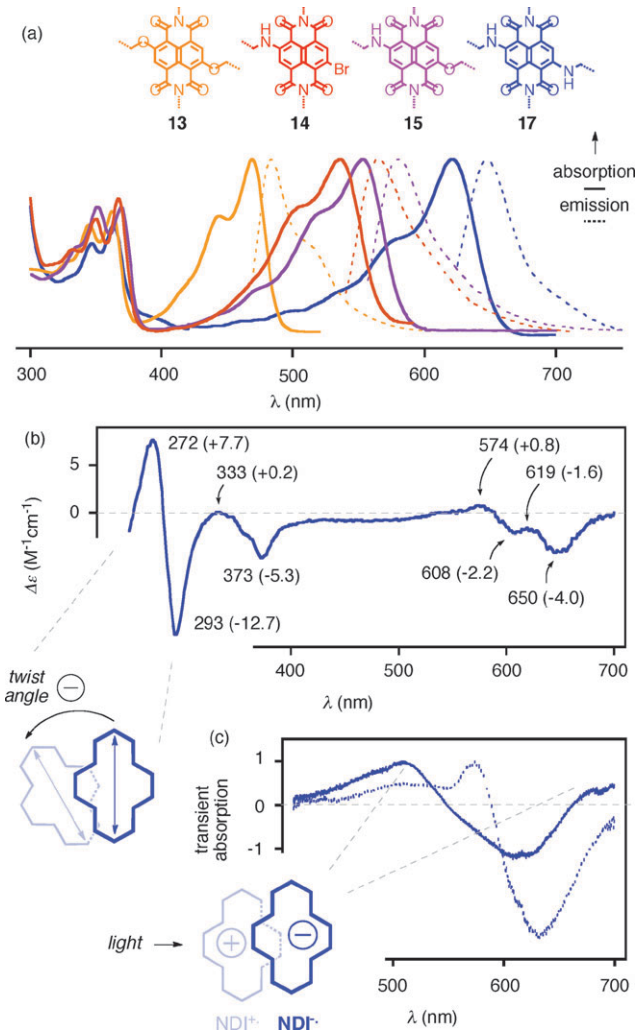

Fig. 3 (a) Absorption (solid) and emission spectra (dashed) of cNDIs **13**, **14**, **15** and **17**, (b) circular dichroism (CD) spectrum of helical stacks of cNDIs **17**, and (c) transient absorption (TA) spectrum of monomeric (dotted) and oligomeric cNDIs **17** (solid). (a) Adapted with permission from ref. 15. Copyright 2009 American Chemical Society. (b) Adapted with permission from ref. 37. Copyright 2006, Wiley. (c) From ref. 16. Reprinted with permission from AAAS.

of radical anions of yellow,[15] red[24,38,39] and blue[40] cNDIs have been observed in combination with nearby hole acceptors or electron donors (see below).

Supramolecular chemistry

The supramolecular chemistry of cNDIs is determined by the nature of their molecular structure. Their ability to form face-to-face π-stacks is determined by their π-acidity.[11,15] Most aromatics are π-basic, with electron clouds above and below an electron deficient aromatic plane producing a negative quadrupole moment Q_{zz} (Fig. 4a). For example, benzene has $Q_{zz} = -8.5$ B (Buckinghams), pyrene $Q_{zz} = -13.8$ B.[11] The quadrupole inversion to π-acidic aromatics is presumably best known from hexafluorobenzene with $Q_{zz} = +9.5$ B.[41] The π-acidity of unsubstituted NDIs **2** is with the computed $Q_{zz} = +18.6$ B almost twice as large and in the range of the explosive TNT.[41]

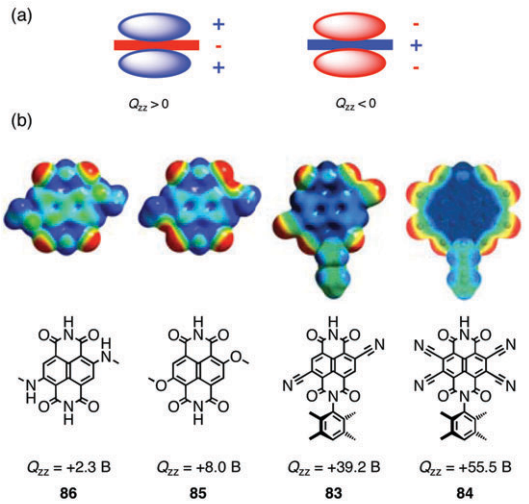

Fig. 4 (a) Schematic side view of π-acidic (left) and π-basic (right) aromatic rings between their electron-poor (blue) and electron-rich (red) π-clouds. (b) Electrostatic potential surfaces (blue positive, red negative) and computed axial quadrupole moments Q_{zz} of cNDIs **83–86**, adapted from ref. 11 and 15 with permission. **83**, **84**: Adapted from ref. 11. Copyright Wiley–VCH Verlag GmbH & Co. KGaA. Reproduced with permission. **85**, **86**: Reproduced with permission from ref. 15. Copyright 2009, American Chemical Society.

The addition of two cyano acceptors in the core of cNDI **83** produces with $Q_{zz} = +39.2$ B exceptional π-acidity (Fig. 4b).[7,11] The electrostatic potential surfaces confirm that the aromatic surface is strongly electron-deficient (deep blue color code). The synthesis of the tetracyano NDI **84** with the highest predicted $Q_{zz} = +55.5$ B has so far not been possible.[7,11] Electron donating core substituents naturally reduce the π-acidity to $Q_{zz} = +8.0$ B for the yellow cNDI **85** and $Q_{zz} = +2.3$ B for the blue cNDI **86**.[15] However, π-acidity is preserved even with two strong amine donors in the core. The quadrupole moment of the green tetraamino cNDIs **18** has not been calculated so far (Fig. 1).

In general, the high π-acidity of cNDIs is ideal for face-to-face π-stacking, binding and transport of anions, and binding and transport of electrons (see below). Molecular models of face-to-face dimers of the yellow cNDI **85** gave with $E_{int} = -27.2$ kcal mol^{-1} interaction energies that are well beyond G–C pairs in DNA duplexes (-19.0 kcal mol^{-1}), not to speak of simple hexafluorobenzene sandwiches (-1.7 kcal mol^{-1}, Fig. 5).[15] The only experimental values available are dissociation constants up to $K_D = 4.1$ mM for unsubstituted NDI dimers with solubilizing peripheral substituents in water.[42] Very small compared to unsubstituted PDIs under similar conditions, these values confirm that cooperative NDI stacking is needed to build stable π-stacks, a situation that is ideal for the construction of supramolecular functional architectures (see below).[43]

In optimized geometries of dimeric model systems, the twist of the aromatic planes was 44°. The short interplane distance of $d = 3.36$ Å was in agreement with very strong interactions. The π–π-interactions between more π-acidic cNDIs are expected to be even stronger.

This journal is © The Royal Society of Chemistry 2010

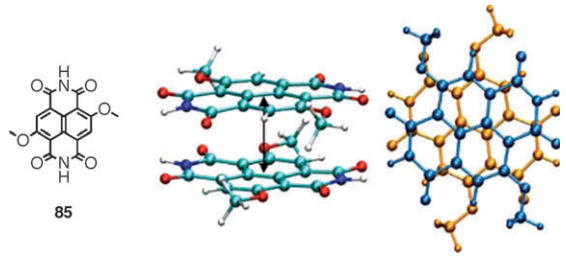

Fig. 5 Molecular model of a face-to-face dimeric complex of **85** viewed from the side (left) and from the top (right). Adapted with permission from ref. 15. Copyright 2009, American Chemical Society.

The second key interaction that dominates self-assembly and self-organization between cNDIs are peripheral hydrogen bonds between primary imide modules as classical acceptor–donor–acceptor (ADA) modules (Fig. 6). However, self-assembly is limited to AD-DA pairing into linear supramolecular polymeric tapes such as **87**.[44] The unused acceptor in each pair accounts for the possibility to yield *trans*- and *cis*-arrangements from the trimer level onward. STM images of monolayers formed by self-assembled cNDI tapes **87** show *cis*/*trans* aligned strings of cNDIs separated by interdigitating alkyl chains (Fig. 7).

Melamine units as classical DAD-partners of ADA-motifs have been used to arrange green cNDIs into supramolecular rosettes **88**.[45] These rosettes have been directly imaged on surfaces. The OPV electron donors attached to the melamine units suggest that rosettes **88** should function as supramolecular donor–acceptor photosystems (see below).

Molecular recognition

Some pioneering examples exist on the usefulness of cNDIs to bind and sense different molecules and ions (Fig. 8). The cyclic 2,3-diamido cNDI **49** has been suggested for use as a colorimetric

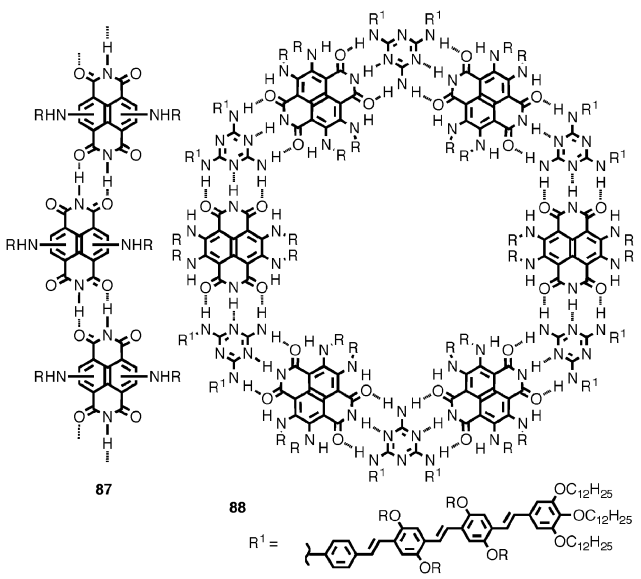

Fig. 6 Self-assembly of cNDIs into supramolecular tapes and programmed assembly into supramolecular rosettes.

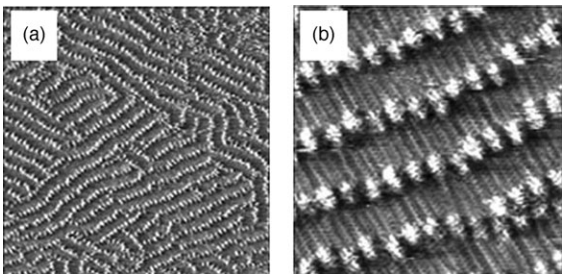

Fig. 7 Large-scale (a, 60 × 60 nm^2) and small-scale (b, 13 × 13 nm^2) STM images of self-assembled cNDI monolayers **87** at the liquid/solid interface. The lines between the cNDI tapes are interdigitating alkyl chains R. Adapted with permission from ref. 44 by permission of The Royal Society of Chemistry.

pH sensor.[29] Absorbing at 454 nm in neutral form, a new maximum at 550 nm was found under basic conditions (Table 1, entry 22). This bathochromic effect can be attributed to the conjugated resonance form **89**, which can further aromatize in the pyrazine tautomer **90**. This stabilization by aromatization might further account for the high acidity of one amide in **49**.

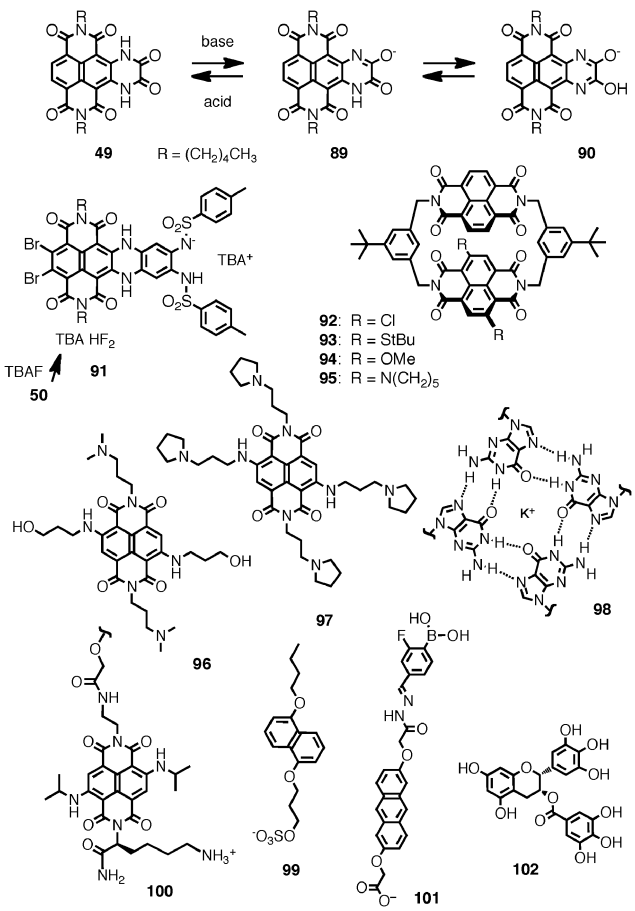

Fig. 8 Molecular recognition and sensing applications of cNDIs include pH sensors **49**, fluoride sensors **50**, and macrocyclic chirality sensors **92–95** as well as the recognition of G-quartets **98** and π-basic intercalators **99** and **101**, the latter to sense polyphenols such as epigallocatechin gallate **102** (see Fig. 13 for full structure of **100**).

The 2,3-expanded cNDI **50** serves as colorimetric fluoride sensors for similar reasons.[30] In the presence of TBAF, the absorption of cNDI **50** at ~615 nm shifts to ~715 nm (Table 1, entry 23). This bathochromic effect has been explained by deprotonation of the tosylamide by the basic fluoride to give complex **91**. The cNDI cyclophanes **92–95** are interesting for sensing applications because they are chiral.[46] The presence of two different NDIs in the macrocycle, one unsubstituted NDI and one cNDI of different color, produces an interesting example of planar chirality. The racemic mixtures could be resolved by chiral HPLC and the CD spectra of the enantiomers are mirror images as expected. The crystal structures reveal intermolecular face-to-face π–π-interactions as well as a preference for heterodimeric intermolecular face-to-face π-stacks between one NDI and one cNDI.

A series of blue cNDIs including **96** and **97** were designed to bind on top and on the bottom of trimeric stacks of G-quartets **98**.[47–49] Crystal structures of complexes of **96** with telomeric DNA reveal the molecular basis of this interesting example for molecular recognition, including face-to-face π–π-interactions on all available G-quartet surfaces but no intercalation into the potassium-templated G-quartet stacks (Fig. 9a).[47] The red emission of cNDIs **97** could be used to directly follow their uptake into the nucleus of MCF7 cells by fluorescence confocal microscopy to bind to telomeric DNA (Fig. 9b).[48] The coinciding recognition of quadruplex sites in the promotor gene of the proto-oncogene KIT, a tyrosine kinase receptor, has been highlighted in a dual quadruplex targeting concept for the treatment of human gastrointestinal stromal tumors (GIST).[49]

Aromatic donor–acceptor interactions supported by ion pairing have been envisioned to make the π-basic dialkoxynaphthalene **99** intercalate into artificial photosystems formed by transmembrane stacks of blue cNDIs **100**.[16] The intercalation of ligand **99** was expected to increase the stack repeat to untwist the helical photosystem into a barrel-stave architecture with ion channel activity (see below). The intercalation of not only π-basic dialkoxynaphthalenes such as **99** but also dialkoxyanthracenes such as **101** into stacks or tweezers of π-acidic NDIs gives pink colored charge-transfer complexes.[8,12,50]

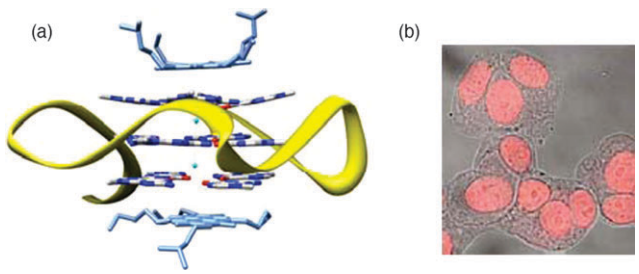

Fig. 9 (a) Side view of the crystal structure of two cNDIs **96** (blue) sandwiching a telomeric quadruplex (atom color code for Gs, yellow ribbon for backbone). The two green spheres are interplane potassium cations. Reproduced from ref. 47, with permission from Elsevier. (b) Fluorescence emission of blue cNDIs **97** accumulating in the nucleus of MCF7 cells. Reproduced from ref. 48, with permission from Elsevier.

The intercalation of dialkoxyanthracene **101** has been used to sense polyphenols such as epigallocatechin gallate **102** within synthetic pores with internal NDI tweezers.[51] The use of anion–π interactions with cNDIs to bind and transport anions will be discussed in the following chapter.[7]

Anion transport

Contrary to the ubiquitous use of cation–π interactions for recognition and catalysis in chemistry and biology,[52] the recognition of anions by anion–π interactions on π-acidic aromatic surfaces has remained mainly a topic in theoretical chemistry.[41,53–57] The high π-acidity of cNDIs suggests that anion–π interactions, if they exist, should be strong.[11] The series of minimalist NDI models **103–106** was prepared to explore the occurrence of anion–π interactions as well as their relevance for function (Fig. 10).[7] In NDIs **103–106**, the π-acidity increases with cyano substituents in the core, whereas the crowding of the active site on the pyridinedione heterocycle decreases with removal of the *ortho*-methyls in the peripheral mesitylenes, and no additional functional groups are present for anions to bind to and generate misleading results.

Direct evidence for anion binding to NDIs **103–106** was obtained by laser-induced tandem ESI-MS-MS fragmentations of heterodimers with a bound chloride anion.[7] The obtained affinity sequence **106** > **105** > **104** > **103** matched expectations from π-acidity and active-site decrowding, binding energies from computational simulations, absorption from charge-transfer complexes, and the ability to act as anion transporter[57–61] in lipid bilayer membranes. With nanomolar effective concentrations, the transport activity of the ideal cNDI **106** is significant, as is the found selectivity toward size and nature of the transported anion. The anti-Hofmeister selectivity found for all NDI transporters supports strong binding to active suprastructures. Nitrate selectivity among oxyanions implies contributions from π–π-interactions to anion binding in NDI dimers. These results demonstrate the functional relevance of anion–π interactions. Considering that anionic reactive intermediates such as enolates should be similarly recognized on asymmetric π-acidic surfaces, the impact of anion–π interactions on organocatalysis is expected to be significant.[7]

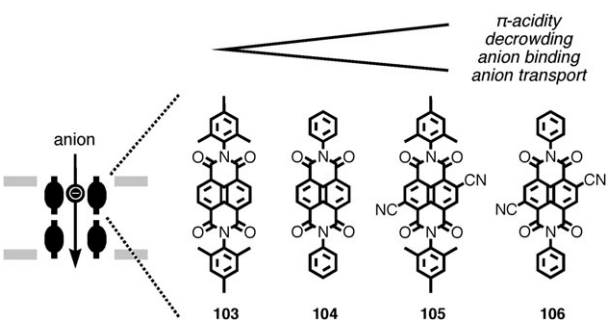

Fig. 10 Structure of NDIs and cNDIs **103–106** used to demonstrate the functional relevance of anion–π interactions with regard to anion binding and transport across lipid bilayer membranes.

This journal is © The Royal Society of Chemistry 2010

Electron transport

The ability of unsubstituted NDIs to transport electrons has been recognized well before anion transport. Pioneering work from the Miller group has confirmed the existence of delocalized radical anions in NDI π-stacks.[62] Later on, unsubstituted NDIs have been identified as one of the few existing air-stable n-semiconductors.[63,64] Strongly dependent on sample preparation, charge mobilities up to 0.10 $cm^2\ V^{-1}\ s^{-1}$ have been observed.

The decreasing LUMO with electron-withdrawing substituents in the core suggests that cNDIs should afford even better n-semiconductors.[6,65,66] To test this hypothesis, top-contact organic field-emitting transistors (OFET) were prepared by using the vapor deposited cNDIs **37** and **11** with one and two cyano acceptors in the core, respectively (Fig. 11; Table 1, entries 3 and 4, R = C_8H_{17}).[6,65,66] Compared to monocyano cNDI **37**, much higher charge mobility was found with dicyano cNDIs **11** in ambient atmosphere (0.11 $cm^2\ V^{-1}\ s^{-1}$) as well as in vacuum (0.15 *vs.* 4.7 × 10^{-3} $cm^2\ V^{-1}\ s^{-1}$). The XRD data obtained with cNDIs **11** and **37** were very similar and indicated, consistent with the undistorted cNDI cores, highly ordered structures. Thus the difference in in-plane ordering is the likely cause of different charge mobilities. Comparison of the charge mobilities obtained with cNDIs and cPDIs under vacuum or in air showed the clear threshold reduction potential (–0.1 V *vs.* SCE), above which the air stability could be attained. With cNDI **11**, air-stable and high mobility OFETs could also be fabricated on overhead transparency films.

To generate n-channel semiconducting polymers with good processability and electron mobilities in ambient conditions for use as organic thin-film transistors (OTFT), polymers of cNDIs with oligothiophene (OT) and related donors in the core have been prepared in several variations (Fig. 11; Table 1, entries 48–55).[19,34] The bandgap of cNDI polymers **76** with bridging bithiophene donors in the core was with 1.45 eV (λ_{max} = 693 nm, Table 1, entry 49) significantly smaller than that of the corresponding cPDI-OT polymers (1.65 eV; λ_{max} = 594 nm). This finding confirms better (more extended) conjugation between cNDIs and oligothiophenes, thanks to the planar aromatic core of cNDIs. The LUMO energy of the cNDI-OT polymer **76** (−3.91 eV; −3.96 eV for cPDI analog) is at the borderline for TFT ambient operation. Bottom-gate top-contact OTFT prepared with these polymers showed

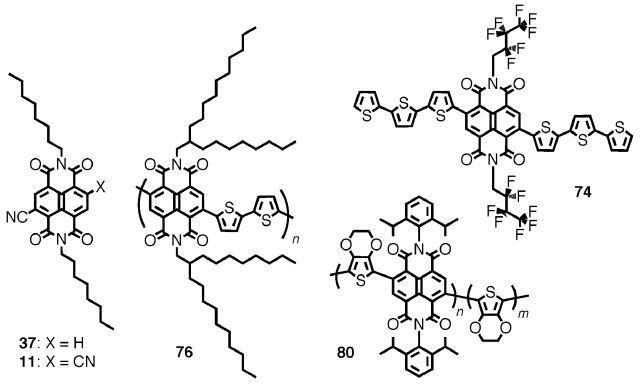

Fig. 11 Important cNDI motifs in studies on electron transport.

n-channel semiconducting properties. Unlike those of cPDI-OT polymers, electron mobilities of the cNDI-OT polymer **76** did not significantly drop (∼0.06 to ∼0.01 $cm^2\ V^{-1}\ s^{-1}$) in the ambient conditions even after 14 weeks. By changing to bottom-contact top-gate TFT with polymeric dielectrics, the charge mobilities with cNDI-OT polymer **76** further improved to 0.45–0.85 $cm^2\ V^{-1}\ s^{-1}$. Consistent with the amorphous nature of cNDI-OT polymer **76**, OTFT performance was not affected by variation of molecular weight, polydispersity or even the deposition techniques (spin-coating or gravure-, flexographic- or inkjet printing).

Compared to cNDI-OT polymer **76**, cNDI-OT polymer **75** with only one bridging thiophene in the core was characterized by an increased bandgap (1.66 eV, λ_{max} = 568 nm) and slightly lower lying HOMO and LUMO energies (Table 1, entry 48).[33] The optoelectronic properties of cNDI-OT polymer **76** were nearly insensitive to changes of the diimide substituents. Addition of head-to-head dodecyl tails to the bithiophene donor increased bandgap and lowered the HOMO level of polymer **77**, whereas the LUMO was not affected (Table 1, entry 50). This significant hypsochromic effect (**77**, λ_{max} = 539 nm; **76**, λ_{max} = 693 nm) originates from non-planarity of head-to-head alkylated thiophenes. However, increased HOMOs of bithiophene donor with head-to-head alkoxy substituents were reflected in polymer **78** with a dramatic bathochromic effect (λ_{max} = 985 nm), a correspondingly narrowed bandgap (1.08 eV) and a very high HOMO (−4.84 eV) with unchanged LUMO (−3.76 eV, Table 1, entry 51). Interestingly, unsubstituted NDIs **2** were shown to form blue charge-transfer complexes with alkoxy-substituted bithiophenes. Taken together, these trends suggest that the bandgap of cNDI-OT polymers is controlled by the π-basicity of the electron-rich oligothiophene donor. Wide-angle X-ray diffraction patterns of cNDI-OT polymers **78** and **76** are consistent with π-stacking (∼4 Å), while **77** gave amorphous material.

The series of cNDIs **72–74** features four oligothiophenes in the core and short fluorocarbon chains in the periphery (Fig. 11; Table 1, entries 45–47).[32] With increasing number of thiophenes in the core, absorption maxima moves to the red up to λ_{max} = 664 nm for **74**. The narrowing of HOMO/LUMO gaps originated mainly from a gradually increasing HOMO level up to −5.36 eV for **74**. HOMO energies obtained from ultraviolet photoemission spectroscopy are shown to match CV data. In bottom-gate OFETs of cNDIs **72–74**, both n-type field effect mobility and on/off ratio decreased with increasing thiophene units, whereas p-type mobility increased. As a result, the device made from **74** exhibited ambipolar behavior (on-off-on with increasing voltage).

The replacement of the central thiophene in cNDI-OT polymers **81** with a fluorene in the fluorescent cNDI-OT polymers **82** has relatively little effect on the narrow bandgap (λ_{max} = 613 nm), indicating that strong electronic interactions along the polymer chain are preserved (Table 1, entries 54 and 55).[36]

A further increase of the HOMO of cNDI-OT polymers **78** with one alkoxy substituent per thiophene calls for dialkoxylated thiophenes.[35] With PEDOT being a standard hole transporting material in most organic solar cells,[67,68] the 3,4-ethylenedioxy (EDO) substituent is the classical choice for this purpose.

The cNDI-EDOT polymers **79** and **80** were prepared by Stille-type polymerization with yields around 60%. The obtained polymers show the expected narrow bandgap. The HOMO and LUMO energy levels support good electronic coupling between the electron donating and accepting units. Polymer solar cells were fabricated with a structure of ITO/poly(3-decylthiophene)/poly(cNDI-EDOT)s (**80**)/2,9-dimethyl-4,7-diphenyl-1,10-phenanthroline (BCP)/Ag. Under white-light illumination (AM 1.5 solar simulator, 100 mW cm^{-2}), the double heterojunction device has an open circuit voltage (V_{oc}) of 0.30 V, a short-circuit current density (J_{sc}) of 2.1 mA cm^{-2} and a fill factor (FF) of 0.24. This calculates to an efficiency of $\sim$0.15%.[35] The efficiency of the best organic solar cells is around 5%.[69–76]

The successful fabrication of organic solar cells with cNDI-EDOT polymers **80** is the first example where the ability of π-stacked cNDIs to transport electrons is combined with light. A summary of photo-induced electron transport with molecular (rather than macromolecular)[35] cNDIs and their supramolecular architectures follows in the next section.

Photoinduced electron transport

The ability to come in all colors on the one hand and transport electrons on the other suggests that cNDIs would be ideal for the construction of artificial photosystems.[25] Several studies in this direction have been published.

The $Ru(bpy)_3$-cNDI-$Ru(bpy)_3$ system **107** has been synthesized to study the effect of electronic coupling between electron donor and acceptor (Fig. 12).[77] The fluorescence lifetime of **107** is with 30 ps much shorter than for control $Ru(bpy)_3$-cNDI dyad **108** (63 ns). This suggests that electron transfer from the excited $Ru(bpy)_3$ donor to the cNDI acceptor is more than a 1000 times faster when $Ru(bpy)_3$ is attached to the core rather than to the periphery. This confirms the importance of electronic coupling for ultrafast photoinduced electron transfer. By the transient absorption of **107**, the rate constant of cNDI radical anion formation (53 ps) could be determined despite the ultrafast recombination (14 ps), while for **108**, photoinduced charge separation was not detected.

Rainbow cNDIs have been coupled with zinc chlorins to harvest light at the periphery of zinc chlorin rod antennas and transfer the photonic energy to the chlorophyll centers.[78,79] The introduction of blue cNDIs **17** was of particular interest to bridge an otherwise unavoidable gap in the visible spectrum. The multichromophoric systems **109**, **110** and **111** have been synthesized by coupling chlorins and cNDIs *via* an esterification followed by metalation of the chlorin center with zinc acetate. Their self-assembly into rod-like structures is driven by non-covalent interactions between the zinc chlorins, whereas the cNDIs at the periphery of the rod antennae do not aggregate. Excitation of these peripheral cNDIs leads to quantitative Förster resonance energy transfer (FRET) to the zinc chlorin acceptors on the picosecond time scale. Compared to native zinc chlorin rods, the light-harvesting efficiency increases by 26% for dyad **110** and 63% for triad **111**.

The artificial photosystem **100** is a tetrameric *M*-helix that is long enough to span a lipid bilayer membrane (Fig. 13).[16] It is composed of π-stacks of blue cNDIs built along *p*-oligophenyl

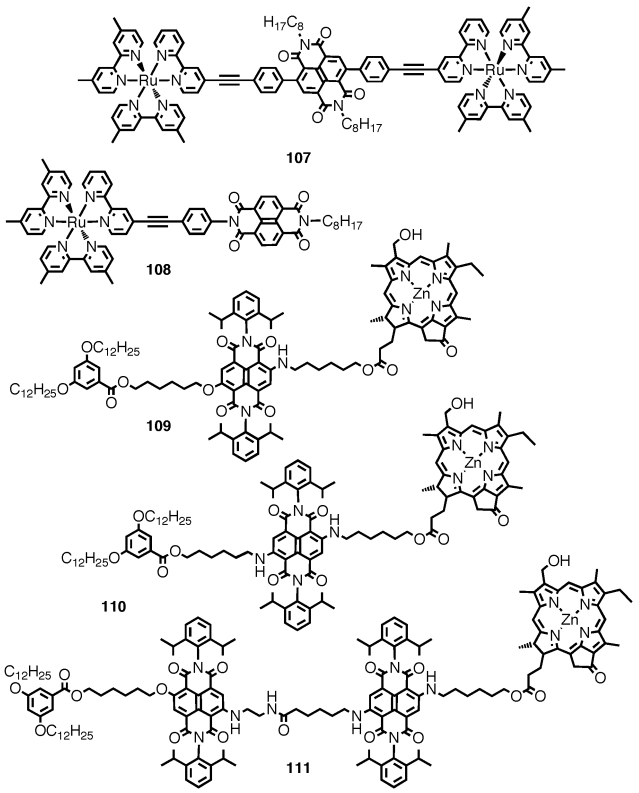

Fig. 12 Important cNDI motifs in studies on photoinduced electron transport.

(POP) rods. In monomeric POP-cNDI systems, the blue chromophores can undergo symmetry-breaking ultrafast and quantitative photoinduced charge separation with a lifetime of 61 ps (Fig. 3c). In the self-assembled artificial photosystem **100**, this lifetime increases to 400 ns.[39]

Photosynthetic activity of photosystem **100** was measured in vesicles loaded with a water-soluble quinone acceptors and a fluorescent pH probe.[16] Excitation of cNDIs followed by photoinduced charge separation initiates electron transfer to the internal quinone acceptor, whereas the hole left behind is filled by external EDTA donors. The consumption of protons during quinone reduction is then detected as a change in pH, and the velocity of the build-up of transmembrane pH gradients with light reports on photosynthetic activity. The Hill plot obtained for photosystem **100** confirmed the tetrameric nature of the active structure.

Photosystem **100** can open up into ion channel **112** in response to the intercalation of ligand **99** into the twisted cNDI stack. This intercalation increases the repeat distance of the π-stack to match the repeat in the POP scaffold. The result is a highly cooperative untwisting of the closed helical architecture into a barrel-stave supramolecular with an internal hydrophilic channel. In single-molecule conductance experiments, this channel is surprisingly homogenous and as small, ohmic and anion selective as designed.[16]

Zipper assembly was introduced to build artificial photosystems with multicolor cNDIs on solid substrates (Fig. 14).[78] These architectures have been well studied and in many variations.[15,24,38,80–85] Without going into details, zipper

 This journal is © The Royal Society of Chemistry 2010

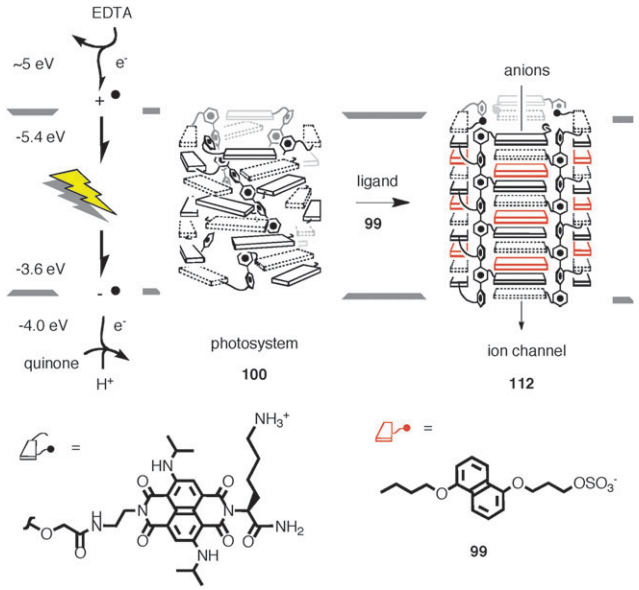

Fig. 13 Artificial photosystems in lipid bilayer membranes that can open up into ion channels in response to chemical stimulation.

assemblies have smoother surfaces, better critical thickness and generate more photocurrents than comparable architectures, and they respond to functional controls.

In zipper assembly, initiators such as **113** are deposited on the surface. This initiator is composed of a short POP scaffold that is decorated with four anionic NDI acceptors. A strained disulfide is placed at one end of the scaffold to react with gold surfaces. The obtained Au-**113** monolayers are then dipped into solutions of propagators such as **114**. The POP scaffold in this propagator is twice as long as in the initiator and decorated with yellow and cationic cNDIs. Directed by intrastack hydrogen-bonded chains and interstack ion pairs, the lower half of these cNDIs forms π-stacks with the NDIs of the initiator, whereas the upper half remains free as sticky ends on the surface to zip up with the anionic propagators **115**, whose sticky ends in turn can zip up the cationic propagators **114**, and so on. The resulting Au-**113**-(**114**-**115**)$_n$ architecture excels with interdigitating intra- and interlayer recognition motifs to align electron-transporting cNDI stacks along strings of hole transporting POP rods. This co-axial alignment of e- and h-transporting channels is referred to as supramolecular n/p-heterojunction (SHJ). SHJs are thought to unify advantages of bilayer (high charge mobility) and bulk n/p-heterojunction (BHJ) organic photovoltaics (OPVs; high charge separation at large donor/acceptor interfaces) and considered as one of the key challenges in current optoelectronics.[25,75,86–90]

In the most advanced photosystem zipped up until now, the obtained yellow SHJ architectures Au-**113**-(**114**-**115**)$_n$ are covered with red oligo-phenylethynyl (OPE) zippers (Fig. 14).[85] The red cNDIs placed on top of the yellow cNDIs create a redox gradient in the e-channel that directs the electrons toward the gold surface. The OPE rods on top of the POP rods create another redox gradient in the h-channel that directs the holes in the other direction toward the surface. As in biological photosystems, these antiparallel redox gradients should direct holes and electrons in opposite directions as soon as they are

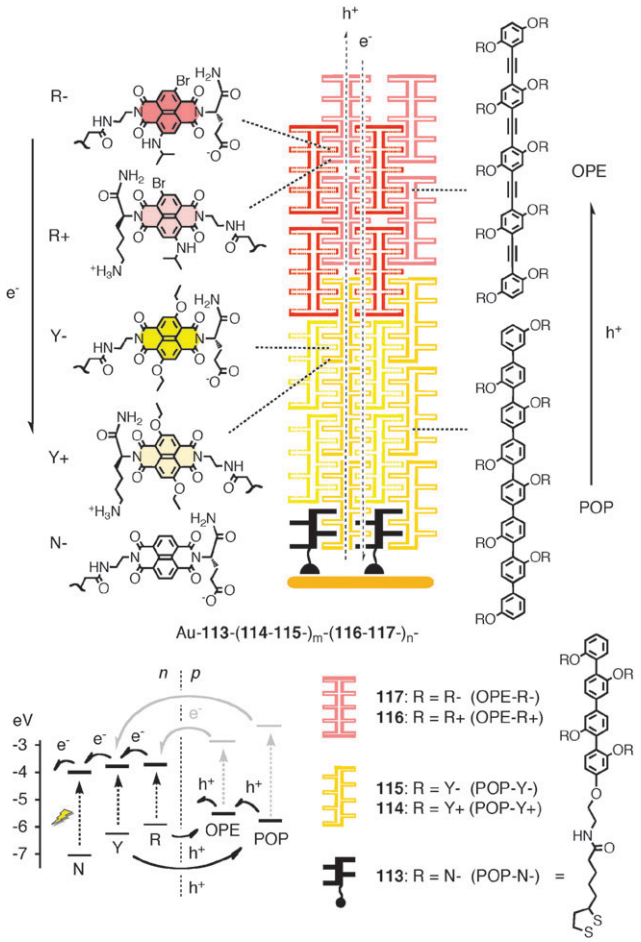

Fig. 14 OMARG-SHJ photosystems on gold with energy levels of the involved components. Here, yellow and red cNDIs are used to harvest light, to inject holes into the nearby acceptors, and to transport electrons in a directional manner.

generated with light and separated at the SHJ interface to never meet each other again and recombine. SHJ architectures with oriented multicolored antiparallel redox gradients have been referred to as OMARG-SHJ. Au-**113**-(**114**-**115**)$_n$-(**116**-**117**)$_n$ is the first example of a minimalist OMARG-SHJ, the reported results satisfy highest expectations.[85]

Perspectives

In summary, research on core-substituted NDIs has experienced recent rapid growth due to mainly breakthroughs with regard to their synthesis and fluorescence. These adventures in new territories are exciting yet still fragmentary and eclectic, covering domains reaching from organic synthesis, supramolecular chemistry and photophysics to applications in materials sciences, biology and medicine. Much input from fundamental studies will be needed to complete the picture. Most important, however, is that the emerging perspectives are very broad and very attractive. The potential to build a broad variety of new (opto)electronic devices is obvious from the results available today (Fig. 1 and 10–14, Table 1). Just to mention a few of the more exotic perspectives, it would be fantastic to have a collection of fluorescent cNDI rainbow

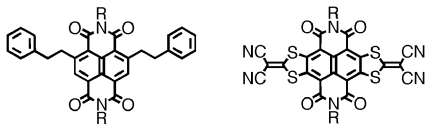

118 119

Fig. 15 Structure of the most recent cNDIs **118** and **119**.

probes in hand for cellular uptake, targeted labeling and multicomponent sensing *in vivo* (Fig. 9b), or to use asymmetric π-acidic cNDI surfaces for organocatalysis with anion–π interactions (Fig. 10).

Breaking news

After submission of this review, two papers appeared describing new cNDIs (**118** and **119**, Fig. 15).[91,92] Particularly noteworthy are the "asymmetric" 2,7-substitution pattern of **118** and the high electron mobility (0.51 $cm^2\ V^{-1}$) observed with the solution processed and ambient stable organic thin film transistor fabricated with **119**. Their photo-electrochemical properties are as follows: **118**: λ_{max} 390 nm, ε 14.0 $mM^{-1}\ cm^{-1}$, λ_{em} 415 nm, QY 0.05%, E_{red} −0.61 V (*vs.* SCE), LUMO −3.8 eV;[91] **119**: λ_{max} 578 nm, E_{red} −0.10 V (*vs.* SCE), LUMO −4.3 eV, HOMO −6.8 eV.[92]

Acknowledgements

This work was supported by the Swiss National Supercomputing Center (CSCS), University of Geneva and the Swiss NSF. We warmly thank all past and present co-workers and collaborators for their contributions to research on this colorful family of molecules.

References

1 H. Vollmann, H. Becker, M. Corell and H. Streeck, *Liebigs Ann.*, 1937, **531**, 1–159.
2 F. Würthner, S. Ahmed, C. Thalacker and T. Debaerdemaeker, *Chem.–Eur. J.*, 2002, **8**, 4742–4750.
3 C. Thalacker, C. Röger and F. Würthner, *J. Org. Chem.*, 2006, **71**, 8098–8105.
4 M. Könemann, *PCT Int. Appl.*, WO 2007074137, 2007.
5 R. S. K. Kishore, V. Ravikumar, G. Bernardinelli, N. Sakai and S. Matile, *J. Org. Chem.*, 2008, **73**, 738–740.
6 B. A. Jones, A. Facchetti, M. R. Wasielewski and T. J. Marks, *J. Am. Chem. Soc.*, 2007, **129**, 15259–15278.
7 R. E. Dawson, A. Hennig, D. P. Weimann, D. Emery, S. Gabutti, J. Montenegro, V. Ravikumar, M. Mayor, J. Mareda, C. A. Schalley and S. Matile, *Nat. Chem.*, 2010, DOI: 10.1038/NCHEM.657.
8 S. V. Bhosale, C. H. Jani and S. J. Langford, *Chem. Soc. Rev.*, 2008, **37**, 331–342.
9 F. Würthner, *Chem. Commun.*, 2004, 1564–1579.
10 K. A. McMenimen and D. G. Hamilton, *J. Am. Chem. Soc.*, 2001, **123**, 6453–6454.
11 J. Mareda and S. Matile, *Chem.–Eur. J.*, 2009, **15**, 28–37.
12 R. S. Lokey and B. L. Iverson, *Nature*, 1995, **375**, 303–305.
13 L. A. Bagatolli, *Biochim. Biophys. Acta*, 2006, **1758**, 1541–1556.
14 R. P. Haugland, *The Handbook. A Guide to Fluorescent Probes and Labeling Techniques*, Invitrogen, Eugene, OR, 10th edn, 2005.
15 R. S. K. Kishore, O. Kel, N. Banerji, D. Emery, G. Bollot, J. Mareda, A. Gomez-Casado, P. Jonkheijm, J. Huskens, P. Maroni, M. Borkovec, E. Vauthey, N. Sakai and S. Matile, *J. Am. Chem. Soc.*, 2009, **131**, 11106–11116.
16 S. Bhosale, A. L. Sisson, P. Talukdar, A. Fürstenberg, N. Banerji, E. Vauthey, G. Bollot, J. Mareda, C. Röger, F. Würthner, N. Sakai and S. Matile, *Science*, 2006, **313**, 84–86.
17 S. Bhosale, M. Kalyankar, S. Bhosale, S. J. Langford, E. Reid and C. Hogan, *New J. Chem.*, 2009, **33**, 2409–2413.
18 S. Chopin, F. Chaignon, E. Blart and F. Odobel, *J. Mater. Chem.*, 2007, **17**, 4139–4146.
19 H. Yan, Z. Chen, Y. Zheng, C. Newman, J. R. Quinn, F. Doetz, M. Kastler and A. Facchetti, *Nature*, 2009, **457**, 679–686.
20 C. Röger and F. Würthner, *J. Org. Chem.*, 2007, **72**, 8070–8075.
21 C. Röger, S. Ahmed and F. Würthner, *Synthesis*, 2007, 1872–1876.
22 X. Gao, W. Qiu, X. Yang, Y. Liu, Y. Wang, H. Zhang, T. Qi, Y. Liu, K. Lu, C. Du, Z. Shuai, G. Yu and D. Zhu, *Org. Lett.*, 2007, **9**, 3917–3920.
23 E. T. Chernick, M. J. Ahrens, K. A. Scheidt and M. R. Wasielewski, *J. Org. Chem.*, 2005, **70**, 1486–1489.
24 R. Bhosale, R. S. K. Kishore, V. Ravikumar, O. Kel, E. Vauthey, N. Sakai and S. Matile, *Chem. Sci.*, 2010, DOI: 10.1039/c0sc00177e.
25 R. Bhosale, J. Misek, N. Sakai and S. Matile, *Chem. Soc. Rev.*, 2010, **39**, 138–149.
26 A. Blaszczyk, M. Fischer, C. von Hänisch and M. Mayor, *Helv. Chim. Acta*, 2006, **89**, 1986–2005.
27 T. Bell, S. Yap, C. Jani, S. Bhosale, J. Hofkens, F. De Schryver, S. J. Langford and K. Ghiggino, *Chem.–Asian J.*, 2009, **4**, 1542–1550.
28 H. Langhals and H. Jaschke, *Chem.–Eur. J.*, 2006, **12**, 2815–2824.
29 F. Doria, M. Di Antonio, M. Benotti, D. Verga and M. Freccero, *J. Org. Chem.*, 2009, **74**, 8616–8625.
30 S. Bhosale, S. Bhosale, M. Kalyankar and S. J. Langford, *Org. Lett.*, 2009, **11**, 5418–5421.
31 S. Suraru and F. Würthner, *Synthesis*, 2009, 1841–1845.
32 H. Krüger, S. Janietz, D. Sainova, D. Dobreva, N. Koch and A. Vollmer, *Adv. Funct. Mater.*, 2007, **17**, 3715–3723.
33 X. Guo and M. D. Watson, *Org. Lett.*, 2008, **10**, 5333–5336.
34 Z. Chen, Y. Zheng, H. Yan and A. Facchetti, *J. Am. Chem. Soc.*, 2009, **131**, 8–9.
35 Y. Wei, Q. Zhang, Y. Jiang and J. Yu, *Macromol. Chem. Phys.*, 2009, **210**, 769–775.
36 P. Piyakulawat, A. Keawprajak, A. Chindaduang, M. Hanusch and U. Asawapirom, *Synth. Met.*, 2009, **159**, 467–472.
37 S. Bhosale and S. Matile, *Chirality*, 2006, **18**, 849–856.
38 R. Bhosale, A. Perez-Velasco, V. Ravikumar, R. S. K. Kishore, O. Kel, A. Gomez-Casado, P. Jonkheijm, J. Huskens, P. Maroni, M. Borkovec, T. Sawada, E. Vauthey, N. Sakai and S. Matile, *Angew. Chem., Int. Ed.*, 2009, **48**, 6461–6464.
39 N. Banerji, A. Fürstenberg, S. Bhosale, A. L. Sisson, N. Sakai, S. Matile and E. Vauthey, *J. Phys. Chem. B*, 2008, **112**, 8912–8922.
40 N. Banerji, G. Duvanel, A. Perez-Velasco, S. Maity, N. Sakai, S. Matile and E. Vauthey, *J. Phys. Chem. A*, 2009, **113**, 8202–8212.
41 B. L. Schottel, H. T. Chifotides and K. R. Dunbar, *Chem. Soc. Rev.*, 2008, **37**, 68–83.
42 M. S. Cubberley and B. L. Iverson, *J. Am. Chem. Soc.*, 2001, **123**, 7560–7563.
43 Z. Chen, A. Lohr, C. R. Saha-Möller and F. Würthner, *Chem. Soc. Rev.*, 2009, **38**, 564–584.
44 C. Thalacker, A. Miura, S. De Feyter, F. C. De Schryver and F. Würthner, *Org. Biomol. Chem.*, 2005, **3**, 414–422.
45 I. De Cat, C. Röger, C. C. Lee, F. J. M. Hoeben, M. J. Pouderoijen, A. P. H. J. Schenning, F. Würthner and S. De Feyter, *Chem. Commun.*, 2008, 5496–5498.
46 S. Gabutti, S. Schaffner, M. Neuburger, M. Fischer, G. Schäfer and M. Mayor, *Org. Biomol. Chem.*, 2009, **7**, 3222–3229.
47 G. N. Parkinson, F. Cuenca and S. Neidle, *J. Mol. Biol.*, 2008, **381**, 1145–1156.
48 F. Cuenca, O. Greciano, M. Gunaratnam, S. Haider, D. Munnur, R. Nanjunda, D. W. Wilson and S. Neidle, *Bioorg. Med. Chem. Lett.*, 2008, **18**, 1668–1673.
49 M. Gunaratnam, S. Swank, S. M. Haider, K. Galesa, A. P. Reszka, M. Beltran, F. Cuenca, J. A. Fletcher and S. Neidle, *J. Med. Chem.*, 2009, **52**, 3774–3783.
50 S. Hagihara, L. Gremaud, G. Bollot, J. Mareda and S. Matile, *J. Am. Chem. Soc.*, 2008, **130**, 4347–4351.
51 S. Hagihara, H. Tanaka and S. Matile, *J. Am. Chem. Soc.*, 2008, **130**, 5656–5657.

 This journal is © The Royal Society of Chemistry 2010

52 J. C. Ma and D. A. Dougherty, *Chem. Rev*., 1997, **97**, 1303–1324.
53 P. Gamez, T. J. Mooibroek, J. S. Teat and J. Reedijk, *Acc. Chem. Res*., 2007, **40**, 435–444.
54 D. Quiñonero, C. Garau, C. Rotger, A. Frontera, P. Ballester, A. Costa and P. M. Deya, *Angew. Chem., Int. Ed*., 2002, **41**, 3389–3392.
55 M. Mascal, A. Armstrong and M. D. Bartberger, *J. Am. Chem. Soc*., 2002, **124**, 6274–6276.
56 I. Alkorta, I. Rozas and J. Elguero, *J. Am. Chem. Soc*., 2002, **124**, 8593–8598.
57 J. T. Davis, P. A. Gale, O. A. Okunola, P. Prados, J. C. Iglesias-Sanchez, T. Torroba and R. Quesada, *Nat. Chem*., 2009, **1**, 138–144.
58 T. M. Fyles, *Chem. Soc. Rev*., 2007, **36**, 335–347.
59 A. P. Davis, N. D. Sheppard and B. D. Smith, *Chem. Soc. Rev*., 2007, **36**, 348–357.
60 G. W. Gokel and N. Barkey, *New J. Chem*., 2009, **33**, 947–963.
61 X. Li, B. Shen, X. Q. Yao and D. Yang, *J. Am. Chem. Soc*., 2009, **131**, 13676–13680.
62 L. L. Miller and K. R. Mann, *Acc. Chem. Res*., 1996, **29**, 417–423.
63 H. E. Katz, A. J. Lovinger, J. Johnson, C. Kloc, T. Siegrist, W. Li, Y. Y. Lin and A. Dodabalapur, *Nature*, 2000, **404**, 478–481.
64 J. M. Warman, M. P. de Haas, G. Dicker, F. C. Grozema, J. Piris and M. G. Debije, *Chem. Mater*., 2004, **16**, 4600–4609.
65 B. A. Jones, A. Facchetti, T. J. Marks and M. R. Wasielewski, *Chem. Mater*., 2007, **19**, 2703–2705.
66 B. A. Jones, A. Facchetti, M. R. Wasielewski and T. J. Marks, *Adv. Funct. Mater*., 2008, **18**, 1329–1339.
67 J. Roncali, P. Blanchard and P. Frère, *J. Mater. Chem*., 2005, **15**, 1589–1610.
68 L. B. Groenendaal, G. Zotti, P.-H. Aubert, S. M. Waybright and J. R. Reynolds, *Adv. Mater*., 2003, **15**, 855–879.
69 J. K. Lee, W. L. Ma, C. J. Brabec, J. Yuen, J. S. Moon, J. Y. Kim, K. Lee, G. C. Bazan and A. J. Heeger, *J. Am. Chem. Soc*., 2008, **130**, 3619–3623.
70 B. C. Thompson and J. M. J. Fréchet, *Angew. Chem., Int. Ed*., 2008, **47**, 58–77.
71 S. Günes, H. Neugebauer and N. S. Sariciftci, *Chem. Rev*., 2007, **107**, 1324–1338.
72 C. Ma, M. Fonrodona, M. C. Schikora, M. M. Wienk, R. A. J. Janssen and P. Bäuerle, *Adv. Funct. Mater*., 2008, **18**, 3323–3331.
73 J.-F. Eckert, J.-F. Nicoud, J.-F. Nierengarten, S.-G. Liu, L. Echegoyen, N. Armaroli, F. Barigelletti, L. Ouali, V. Krasnikov and G. Hadziioannou, *J. Am. Chem. Soc*., 2000, **122**, 7467–7479.
74 N. Martín, L. Sánchez, M. Ángeles Herranz, B. Illescas and D. M. Guldi, *Acc. Chem. Res*., 2007, **40**, 1015–1024.
75 F. Yang, M. Shtein and S. Forrest, *Nat. Mater*., 2005, **4**, 37–41.
76 E. A. Gibson, A. L. Smeigh, L. Le Pleux, J. Fortage, G. Boschloo, E. Blart, Y. Pellegrin, F. Odobel, A. Hagfeldt and L. Hammarström, *Angew. Chem., Int. Ed*., 2009, **48**, 4402–4405.
77 F. Chaignon, M. Falkenstroem, S. Karlsson, E. Blart, F. Odobel and L. Hammarström, *Chem. Commun*., 2007, 64–66.
78 C. Röger, M. G. Mueller, M. Lysetska, Y. Miloslavina, A. R. Holzwarth and F. Würthner, *J. Am. Chem. Soc*., 2006, **128**, 6542–6543.
79 C. Röger, Y. Miloslavina, D. Brunner, A. R. Holzwarth and F. Würthner, *J. Am. Chem. Soc*., 2008, **130**, 5929–5939.
80 N. Sakai, A. L. Sisson, T. Bürgi and S. Matile, *J. Am. Chem. Soc*., 2007, **129**, 15758–15759.
81 A. L. Sisson, N. Sakai, N. Banerji, A. Fürstenberg, E. Vauthey and S. Matile, *Angew. Chem., Int. Ed*., 2008, **47**, 3727–3729.
82 N. Sakai, R. S. K. Kishore and S. Matile, *Org. Biomol. Chem*., 2008, **6**, 3970–3976.
83 M. Lista, N. Sakai and S. Matile, *Supramol. Chem*., 2009, **21**, 238–244.
84 S. Maity, R. Bhosale, N. Banerji, E. Vauthey, N. Sakai and S. Matile, *Org. Biomol. Chem*., 2010, **8**, 1052–1057.
85 N. Sakai, R. Bhosale, D. Emery, J. Mareda and S. Matile, *J. Am. Chem. Soc*., 2010, DOI: 10.1021/ja101944r.
86 F. Würthner, Z. Chen, F. J. M. Hoeben, P. Osswald, C.-C. You, P. Jonkheijm, J. Herrikhuyzen, A. P. H. J. Schenning, P. P. A. M. van der Schoot, E. W. Meijer, E. H. A. Beckers, S. C. J. Meskers and R. A. J. Janssen, *J. Am. Chem. Soc*., 2004, **126**, 10611–10618.
87 A. B. F. Martinson, A. M. Massari, S. J. Lee, R. W. Gurney, K. E. Splan, J. T. Hupp and S. T. Nguyen, *J. Electrochem. Soc*., 2006, **153**, A527–A532.
88 H. J. Snaith, G. L. Whiting, B. Sun, N. C. Greenham, W. T. S. Huck and R. H. Friend, *Nano Lett*., 2005, **5**, 1653–1657.
89 A. Kira, T. Umeyama, Y. Matano, K. Yoshida, S. Isoda, J. K. Park, D. Kim and H. Imahori, *J. Am. Chem. Soc*., 2009, **131**, 3198–3200.
90 Y. Yamamoto, G. Zhang, W. Jin, T. Fukushima, N. Ishii, A. Saeki, S. Seki, S. Tagawa, T. Minari, K. Tsukagoshi and T. Aida, *Proc. Natl. Acad. Sci. U. S. A*., 2009, **106**, 21051–21056.
91 J. E. Bullock, M. T. Vagnini, C. Ramanan, D. T. Co, T. M. Wilson, J. W. Dicke, T. J. Marks and M. R. Wasielewski, *J. Phys. Chem. B*, 2010, **114**, 1794–1802.
92 X. Gao, C. Di, Y. Hu, X. Yang, H. Fan, F. Zhang, Y. Liu, H. Li and D. Zhu, *J. Am. Chem. Soc*., 2010, **132**, 3697–3699.